NeuroImage 291 (2024) 120585

Contents lists available at ScienceDirect

NeuroImage

journal homepage: www.elsevier.com/locate/ynimg

On the interplay between state-dependent reconfigurations of global signal correlation and BOLD fluctuations: An fMRI study

Stefano Damiani [a,1], Paolo La-Torraca-Vittori [a,*,1], Livio Tarchi [b], Eleonora Tosi [a], Valdo Ricca [b], Andrea Scalabrini [c], Pierluigi Politi [a], Paolo Fusar-Poli [a,d,e,f]

[a] Department of Brain and Behavioral Sciences, University of Pavia, Via Bassi 21, Pavia, Italy
[b] Psychiatry Unit, Department of Health Sciences, University of Florence, Florence, Italy
[c] Department of Human and Social Sciences, University of Bergamo, Bergamo, Italy
[d] Department of Psychosis Studies, King's College London, London, UK
[e] Outreach and Support in South-London (OASIS) service, South London and Maudlsey (SLaM) NHS Foundation Trust, UK
[f] Department of Psychiatry and Psychotherapy, Ludwig-Maximilian-University, Munich, Germany

ARTICLE INFO

Keywords:
Global signal
Functional connectivity
Resting state
Stop-signal task
Bold activation
Negative BOLD signals

ABSTRACT

Background: The dynamics of global, state-dependent reconfigurations in brain connectivity are yet unclear. We aimed at assessing reconfigurations of the global signal correlation coefficient (GSCORR), a measure of the connectivity between each voxel timeseries and the global signal, from resting-state to a stop-signal task. The secondary aim was to assess the relationship between GSCORR and blood-oxygen-level-dependent (BOLD) activations or deactivation across three different trial-conditions (GO, STOP-correct, and STOP-incorrect).

Methods: As primary analysis we computed whole-brain, voxel-wise GSCORR during resting-state (GSCORR-rest) and stop-signal task (GSCORR-task) in 107 healthy subjects aged 21–50, deriving GSCORR-shift as GSCORR-task minus GSCORR-rest. GSCORR-tr and trGSCORR-shift were also computed on the task residual time series to quantify the impact of the task-related activity during the trials. To test the secondary aim, brain regions were firstly divided in one cluster showing significant task-related activation and one showing significant deactivation across the three trial conditions. Then, correlations between GSCORR-rest/task/shift and activation/deactivation in the two clusters were computed. As sensitivity analysis, GSCORR-shift was computed on the same sample after performing a global signal regression and GSCORR-rest/task/shift were correlated with the task performance.

Results: Sensory and temporo-parietal regions exhibited a negative GSCORR-shift. Conversely, associative regions (ie. left lingual gyrus, bilateral dorsal posterior cingulate gyrus, cerebellum areas, thalamus, posterolateral parietal cortex) displayed a positive GSCORR-shift (FDR-corrected $p < 0.05$). GSCORR-shift showed similar patterns to trGSCORR-shift (magnitude increased) and after global signal regression (magnitude decreased). Concerning BOLD changes, Brodmann area 6 and inferior parietal lobule showed activation, while posterior parietal lobule, cuneus, precuneus, middle frontal gyrus showed deactivation (FDR-corrected $p < 0.05$). No correlations were found between GSCORR-rest/task/shift and beta-coefficients in the activation cluster, although negative correlations were observed between GSCORR-task and GO/STOP-correct deactivation (Pearson rho=-0.299/-0.273; Bonferroni-$p < 0.05$). Weak associations between GSCORR and task performance were observed (uncorrected $p < 0.05$).

Conclusion: GSCORR state-dependent reconfiguration indicates a reallocation of functional resources to associative areas during stop-signal task. GSCORR, activation and deactivation may represent distinct proxies of brain states with specific neurofunctional relevance.

Abbreviations: GS, global signal; GSR, global signal regression; GSCORR, global signal correlation coefficient.

* Corresponding author.
E-mail address: paolo.latorracavitto01@universitadipavia.it (P. La-Torraca-Vittori).

[1] The authors equally contributed to the study.

https://doi.org/10.1016/j.neuroimage.2024.120585
Received 5 December 2023; Received in revised form 10 March 2024; Accepted 22 March 2024
Available online 23 March 2024

1. Introduction

Human brain functionality is characterized by spatially and temporally correlated low-frequency fluctuations in the blood oxygenation level-dependent (BOLD) signal (Choe et al., 2015). BOLD fluctuations can be assessed via functional Magnetic Resonance Imaging (fMRI), both when the individual is at rest (i.e., resting-state) and during the execution of specific tasks (Ma et al., 2012; Rogers et al., 2007; Scalabrini et al., 2020b). In order to regulate intrinsic brain activity, BOLD fluctuations are functionally organized at local, long-range and global scales, which constantly communicate to generate complex dynamics (Qin et al., 2020). Recent studies attempted to characterize the state-dependent reconfigurations of local and long-range functional connectivity (FC), finding a reduced local connectivity opposed to an increased long-range FC from rest to task (Damiani et al., 2022; Tommasin et al., 2018).

In contrast, the state-dependent reconfiguration of FC dynamics at a global scale has been poorly investigated up to the present date. On a global scale, FC can be measured by the global signal correlation coefficient (GSCORR), that is the correlation between each voxel time series and the averaged global signal (GS) of the gray matter (Ao et al., 2021; Fox et al., 2009; Power et al., 2017; Scalabrini et al., 2020a). For this reason, GSCORR is also referred to as GS topography, representing an emerging measure for analyzing the relationship between global and local neural activities. Developed to gain a deeper understanding of the neurobiological significance of GS, GSCORR exhibits interesting physiological and pathological correlates opening up intriguing new frontiers for the neuroimaging research (Ao et al., 2021). For instance, GSCORR demonstrates an intrinsic architecture characterized by higher values in sensory cortices and lower values in high-order cortices during the resting state (Ao et al., 2021; Li et al., 2020; Power et al., 2017; Zhang et al., 2020). Furthermore, GSCORR has been found to be altered in states of unconsciousness, potentially linking GSCORR to brain states related to vigilance (Tanabe et al., 2020). Moreover, GSCORR was altered in various psychiatric and neurological disorders, such as patients with schizophrenia, major depressive disorder, bipolar disorder, and epilepsy (Li et al., 2020; Scalabrini et al., 2020b; Yang et al., 2016).

Regarding the behavioral correlates of GSCORR in cognitive tasks, to our knowledge, only one study examined the presence of state-dependent changes in GSCORR from rest to task (Zhang et al., 2020). Irrespectively of task design, Zhang and colleagues observed a general GSCORR reduction in the majority of brain regions, especially in somatosensory areas. Of note, these results reported unchanged GSCORR values in brain areas that should have been engaged across tasks. One example is the primary visual cortex, as almost all the tasks evaluated included visual stimuli. However, no direct comparison between GSCORR and task activation was performed, leaving open questions regarding the relationship between these two indexes (Ao et al., 2021).

Given the aforementioned gaps in the literature, the primary aim of this study was to evaluate the state-dependent reconfigurations of global connectivity in a sample of healthy subjects by measuring voxel-wise, within-group differences of GSCORR occurring from rest to a stop-signal task (GSCORR-shift). The secondary objective of this study was to explore the relationship between GSCORR and task-related BOLD changes. To assess this relationship, we mapped the regions with positive and negative changes in the BOLD signal during a stop-signal task and measured the correlation patterns between GSCORR-rest/task/shift and the beta coefficients in these regions.

2. Materials and methods

2.1. Sample - participants

This study analyzed imaging and clinical data of 130 healthy controls adults (HC) from the University of California, Los Angeles (UCLA) Consortium for Neuropsychiatric Phenomics open-access neuroimaging dataset (Gorgolewski et al., 2017; Poldrack et al., 2016). Participants were aged 21–50 years, right-handed and English-speaking. Ethnic category was either White, Hispanic, or Latino. A screening urinalysis was performed, and only individuals negative for drugs of abuse were enrolled (Cocaine; Methamphetamine; Morphine; THC; Benzodiazepines). Subjects were excluded if they had lifetime diagnoses of: Schizophrenia or Other Psychotic Disorder; Bipolar I or II Disorder; Substance Abuse or Dependence (not counting caffeine or nicotine); current Major Depressive Disorder; suicidality; Anxiety Disorder (Obsessive Compulsive Disorder, Panic Disorder, Generalized Anxiety Disorder, Post-Traumatic Stress Disorder), Attention Deficit Hyperactivity Disorder (ADHD). Participants were also excluded if left-handed, believed they might be pregnant, or if had other contraindications to scanning (e.g., claustrophobia, metal in body, body too large to fit in scanner). Further details about recruiting and demographics can be found in two works from Poldrack, Gorgolewski and colleagues (Gorgolewski et al., 2017; Poldrack et al., 2016).

2.2. Informed consent and ethical approval

As described in the original study, participants were given a verbal explanation of the study, after which written informed consent was signed. Procedures were approved by the Institutional Review Boards at UCLA and the Los Angeles County Department of Mental Health (Poldrack et al., 2016).

2.3. Task description

The stop-signal task was chosen for the analysis due to its constant recruitment of attentive resources required across the whole scan-time. This characteristic made stop-signal a continuous task-state which is ideal to be compared to rest. The stop-signal task run lasted 386 s. Participants were instructed to respond as fast as they could after a ‘go’ stimulus was presented on the computer screen, except for the subset of trials where the ‘go’ stimulus was paired with a ‘stop’ signal. Go stimuli consisted of left- and right-wards pointing arrows to which participants were told to respond by pressing the respective button. For stop trials (25 % of total trials), a stop-signal (a 500 Hz tone presented through headphones) was presented with a short delay -stop-signal delay- after the go stimulus appeared and lasted for 250 ms. Participants were instructed to respond as quickly and accurately as possible in all trials, but to withhold their response if they heard the stop-signal. They were also instructed that stopping and going were equally important. Performance was then measured through the Stop-Signal Reaction Time (SSRT), an index based on the horse-race model and considered a critical measure of the cognitive control processes involved in stopping (Logan and Cowan, 1984; Verbruggen and Logan, 2009;2008). SSRT is the time it takes for an individual to inhibit a preplanned action in response to a stop signal. SSRT was computed as the quantile reaction time minus the mean of all stop-signal delay values; longer SSRTs corresponded to worse performances. To yield approximately 50 % successful response inhibition for the estimation of stop-signal reaction time (SSRT), the stop-signal delay of each Stop trial was dynamically adjusted (Band et al., 2003). As additional performance measure, uncorrected, we used mean reaction time (RT) on all correct GO trials as they were collected for each participant.

2.4. Preprocessing

fMRI data were preprocessed with AFNI software (Bowring et al., 2021; Cox, 1996; Cox and Hyde, 1997). The structural and functional reference images were co-registered (Saad et al., 2009). The first 4 frames of each fMRI run were removed to discard the transient effects in amplitude observed until magnetization achieves steady state (Caballero-Gaudes and Reynolds, 2017). Slice timing correction (Konstantareas and Hewitt, 2001) and despike methods (Satterthwaite et al.,

2013) were applied. Rigid-body alignment of the structural and functional image was performed. The anatomical image was then warped to the Montreal Neurological Institute standard space (MNI152_T1_2009c) template provided with the AFNI binaries. Spatial smoothing was applied using a Gaussian filter with full width at half maximum (FWHM) kernel sizes of 6 mm. Bandpass within the standard frequency range (0.01–0.1 Hz) was performed (Shirer et al., 2015). Each of the voxel time series was then scaled to have a mean of 100. To control for non-neural noise, regression based on the 6 rigid body motion parameters and their 6 derivatives was applied, as well as mean time series from cerebro-spinal fluid masks (Fox et al., 2005; Vovk et al., 2011) and eroded by one voxel (Chai et al., 2012). For GSCORR analysis, regression of white matter artifacts was performed through the fast ANATICOR technique provided by AFNI (Jo et al., 2010) to further improve motion correction, censoring of voxels with a Framewise Displacement (FD) above 0.5 mm was applied to the timeseries (Power et al., 2014). A strict control of motion was performed, as subjects with >2 mm or >2° of motion and/or more than 20 % of timepoints above FD 0.5 mm in rest or task run were excluded (Damiani et al., 2022).

2.5. Primary analysis: GSCORR

The global signal (GS) was calculated for each participant by averaging the fMRI signals of all the gray matter voxels. For each voxel, the GS topography (i.e., GSCORR) was calculated as the Pearson correlation coefficient between the time series of the voxel and the GS time series (Fox et al., 2009; Power et al., 2017; Scalabrini et al., 2020b). The Pearson correlation coefficients were computed for the rest and task run and then transformed through Fisher z transformation for statistical analysis (GSCORR-rest and GSCORR-task respectively) (Cole et al., 2016; 2014). Voxel-wise differences between GSCORR-rest and GSCORR-task, i.e. GSCORR-shift, were evaluated through a paired *t*-test (task minus rest). Results were masked using a gray matter mask derived from the MNI template of choice. For all primary and secondary analyses, the significance threshold was False Discovery Rate-corrected p value (FDR-p) of 0.05 with a minimum cluster size > 30 significant voxels, calculated by the three nearest neighbors, to further strengthen the robustness of our results (Zhu et al., 2019).

2.6. Secondary analyses

2.6.1. GSCORR-shift computed as rest – task residual

Fair and colleagues introduced the concept of task residual BOLD activity, suggesting that this measure should represent the spontaneous signal of the brain during a "task state" (Fair et al., 2007). Task residual activity is obtained by removing from the task time-series the task-related activation using a General Linear Model (GLM). As GSCORR was computed using task time-series where task-related activity was not regressed out, to compare GSCORR-task with GSCORR on task residuals (GSCORR-tr) would allow to quantify the impact of the task-related activity during the trials.

After obtaining GSCORR-tr, a *t*-test between GSCORR-tr and GSCORR-rest was performed to obtain task residual GSCORR-shift (trGSCORR-shift). A congruence between GSCORR-shift and trGSCORR-shift maps would confirm the existence of a task-oriented state, characterized by the continuous engagement of attentional resources and readiness to respond, in the context of the stop-signal task. As suggested by Zhang and colleagues, such task-oriented state would be trial-independent (Zhang et al., 2020).

2.6.2. Task activation analysis

We planned to model the following task conditions for each subject: successful "go" condition ("GO"), unsuccessful "go" condition ("MISS"), successful "stop" condition (correct rejection, "STOPcor"), and unsuccessful "stop" condition ("STOPincor"). However, as observed by a previous study, MISS conditions were excluded from the analysis due to the very low number of events per subject (Cao and Cannon, 2021). GO, STOPcor and STOPincor conditions were therefore convolved with a hemodynamic response function and included in a general linear model together with other regressors such as 6 rigid body parameters and their 6 derivatives, mean time series from cerebro-spinal fluid and white matter masks eroded by one voxel and FD-based censoring (see above) at each time point. A gray matter mask was then applied on the resulting activation maps.

In addition to computing BOLD activation with positive beta coefficients, we also considered BOLD deactivation measuring the negative beta coefficients. The physiological basis and precise meaning of negative beta coefficients remains a topic of ongoing debate, and up to the present day the literature has provided insufficient information concerning its dynamics in stop-signal tasks (Nakata et al., 2019). Several mechanisms have been proposed to explain negative beta coefficients, including: (a) the "blood steal" phenomenon, whereby a decrease in blood flow occurs in regions adjacent to activated regions with increased blood flow and supplied by a common artery (Harel et al., 2002; Kannurpatti and Biswal, 2004); (b) the "neural inhibition hypothesis" (Buzsáki et al., 2007; Devor et al., 2008; Shmuel et al., 2002; Sten et al., 2017), according to which negative BOLD responses are caused by local neural inhibition, as a result of interhemispheric transcallosal inhibition (Allison et al., 2000; Hamzei et al., 2002; Stefanovic et al., 2004; Sten et al., 2017; Tzourio-Mazoyer et al., 2015; Yuan et al., 2013; Zeharia et al., 2012) or task-related deactivation of associated areas belonging to an irrelevant sensory modality (Sadato et al., 1998, 1996; Sten et al., 2017). While considering these premises that highlight the functional relevance of negative beta coefficients, for practical reasons we will refer to these values using the term "deactivation".

The clusters of areas that resulted significantly activated or deactivated during the execution of the stop-signal task were extracted as masks. This analysis was performed for the three trial conditions, namely: STOPcor, STOPincor and GO. The surviving clusters of voxels for each trial were overlapped to produce: a) one mask constituted by regions showing activation across the three different conditions; b) one mask constituted by regions showing deactivation across the three different conditions.

2.6.3. GSCORR relationship with task-related changes in BOLD activity

Aside from providing a precise mapping of the regions involved in the processing of stop-signal tasks, the generation of maps across the three conditions allowed to compare GSCORR and task activation measures. In fact, GSCORR is computed across all task states and does not distinguish GO, STOPcor and STOPincor responses. To quantify the level of association between GSCORR and activation/deactivation, the following values were extracted in areas of overlap between activation and deactivation for each subject: a) GO, STOPcor and STOPincor trials beta coefficients; b) GSCORR-rest, GSCORR-task and GSCORR-shift. Finally, Pearson's correlation coefficients were calculated between beta coefficients and GSCORR-rest/task/shift. Bonferroni correction for multiple comparisons was performed. This analysis offered not only the possibility to compare GSCORR with BOLD changes, but also to map the brain regions that are recruited during each of the three task conditions. Finally, to facilitate the topographic comparison between GSCORR-shift and clusters of common activation/deactivation during the task, we created two maps comparing GSCORR-shift with activation and deactivation. The thresholds for this analysis were set at FDR-$p = 0.05$ with a minimum cluster size > 30 significant voxels, calculated by the three nearest neighbors. These maps are available in Supplementary materials (eFig.4).

2.7. Sensitivity analyses: global signal regression (GSR) analysis and performance correlation

(i) Whether preprocessing should include GSR or not is controversial (Murphy and Fox, 2017; Shirer et al., 2015); in particular, GSR was

shown to significantly influence GSCORR analyzes (Scalabrini et al., 2020a, 2020b). In order to account for the GSR effect, primary analyses were repeated after the regression of the gray matter averaged time series. Due to the global nature of the GSCORR index, we expected a reduction or absence of significant findings in the GSR-related analysis.

(ii) In order to evaluate the behavioral correlates of GSCORR, SSRT and RT scores were introduced as covariates using the option -covariate in the 3dttest++ AFNI command to explore how this measure covaried with GSCORR-rest, GSCORR-task, and GSCORR-shift on a voxel-wise level. The -covariate option produced 3 whole-brain maps as output. Each map refers to one of the paired *t*-test parameters (map1: covariance with GSCORR-rest; map2: covariance with GSCORR-task; map3: covariance with GSCORR-shift). Covariance voxel-wise maps thus showed the significant regions of covariance between GSCORR and performance (SSRT and RT). As no significant differences were observed at FDR-$p = 0.05$, uncorrected $p = 0.05$ thresholds were adopted for the results of this explorative analysis. Results are available in Supplementary materials.

3. Results

3.1. Descriptive statistics

23 subjects were excluded from the analyses due to excessive motion in either rest or task run. A total of 107 subjects were finally selected. The sample was composed of 52 % males; had an average age of 30.85 ± 8.6 years; the mean SSRT was 213.28 ± 40.35 ms; the mean RT was 213.28 ± 112.36 ms.

3.2. GSCORR-shift

GSCORR-shift (GSCORR-task vs GSCORR-rest) map is shown in Fig. 1. We found a reduction of GSCORR during task in bilateral insula, bilateral somatosensory cortex, bilateral auditory cortex, bilateral secondary visual network areas, bilateral middle temporal gyrus, bilateral fusiform gyrus, right inferior frontal gyrus. Increased GSCORR values were found in associative areas such as left lingual gyrus, bilateral dorsal posterior cingulate gyrus (dPCC), bilateral cerebellum areas, bilateral thalamus, bilateral posterolateral parietal cortex (PLPC). The trGSCORR-shift map (see Fig. 1) exhibited a very similar pattern to that of GSCORR-shift. Notably, a general enhancement in the signal-to-noise ratio was observed in trGSCORR-shift compared to GSCORR-shift. However, this enhancement was especially relevant in specific clusters of subcortical areas including the cerebellum.

3.3. Task-related BOLD changes

Figs. 2 and 3 display the regions respectively showing activation or deactivation during GO, STOPcor and STOPincor task conditions.

The regions showing activation across all the three trials included left Area 6 of Brodmann (including: supplementary motor areas, SMA; pre-supplementary motor areas, pre-SMA) and inferior parietal lobule (IPL) (including: supra-marginalis gyrus; left superior temporal gyrus).

The regions showing deactivation across all the three trials involved bilateral posterior parietal lobule, bilateral cuneus and bilateral precuneus, left middle frontal gyrus.

While STOP conditions were mainly linked to activations, the GO condition mainly produced deactivation. Activation/deactivation maps for all task conditions have been provided as NIFTI files in the Supplementary materials.

3.4. Relationship between GSCORR and task-related BOLD changes

eFig. 4 shows the conjunction map between GSCORR-shift and areas showing activation/deactivation during the task. GSCORR-shift exhibited minimal overlap with both activation and deactivation clusters. Specifically, a small overlap between negative GSCORR-shift and activation clusters was visible in left Inferior Parietal Lobule (IPL) and left Brodmann area 6. Concerning GSCORR-shift/deactivation overlaps, the map only showed very restricted area in left precuneus (positive GSCORR-shift) and right cuneus (negative GSCORR-shift).

Tables 1A and 1B show correlation analysis between GSCORR values and the beta coefficients for the regions showing either activation or deactivation across all the three task conditions.

We found significant correlations only in areas showing common deactivation, where GSCORR-task values exhibited a negative correlation with GO beta coefficients ($r = -0.299$; uncorrected $p = 0.002$, corrected $p = 0.018$) and STOPcor beta coefficients ($r = -0.273$; uncorrected $p = 0.005$, corrected $p = 0.040$). Marginal significances, not surviving Bonferroni correction, were also found in areas of common deactivation for GO beta coefficients and GSCORR-rest ($r = -0.210$; uncorrected $p = 0.031$), STOPincor and GSCORR-rest ($r = -0.251$; uncorrected $p = 0.013$) and STOPincor and GSCORR-task ($r = -0.198$; $p = 0.042$). Marginally significant correlation was also found in areas showing common activation for STOPcor beta coefficients and GSCORR-shift values ($r = 0.245$; uncorrected $p = 0.011$). See Table 1.

3.5. Sensitivity analyses

The analyses conducted after GSR showed that GSCORR-shift was largely inferior in magnitude compared to the GSCORR-shift measured without GSR (eFig. 1). However, the global pattern was still characterized by a predominance of areas with negative GSCORR-shift. Interestingly, the regions where GSCORR-shift was significant in GSR were almost complementary to the ones observed in the no-GSR analysis.

The covariance analyses between GSCORR-rest/task/shift and SSRT found minimally significant results even when adopting the uncorrected-p threshold of 0.05. However, at the same threshold of uncorrected-$p = 0.05$, RT showed both positive and negative correlations with GSCORR-rest, GSCORR-task, and GSCORR-shift. Voxel-wise findings are reported in eFigs. 2 and 3.

4. Discussion

Our primary findings showed non-uniform, state-dependent GSCORR reconfigurations, highlighting a negative GSCORR-shift (task < rest) in the majority of sensory and temporo-parietal regions, as opposed to a positive GSCORR-shift (task > rest) in associative regions. Although separate regions were involved in the processing of STOP and GO conditions, a few areas were recruited in all the stop-signal trials. Activation in these regions did not correlate to GSCORR-rest/task/shift. Conversely, small but reliable negative associations were observed between deactivation and GSCORR-task.

4.1. State-dependent GSCORR reconfiguration

The primary aim of this study was to evaluate state-dependent reconfigurations of whole-brain, voxel-wise GSCORR. According to the current knowledge, FC reconfiguration dynamics from rest to task involve a generalized reduction in ReHo (Damiani et al., 2022; Tommasin et al., 2018), a reduction in within-network FC (Cole et al., 2019; Tommasin et al., 2018), and an increase in between-networks FC (Cole et al., 2019; Tommasin et al., 2018). The present findings add important information concerning the state-dependency of global connectivity by observing two state-dependent reconfiguration patterns of GSCORR. The first dominant pattern showed widespread GSCORR reductions in somatosensory and auditory regions. This pattern has also been observed by Zhang and colleagues across several tasks, suggesting a common and unspecific trend when transitioning from rest to task states (Zhang et al., 2020).

Nonetheless, the current study is the first to describe a second pattern, that is a GSCORR increase in associative subcortical (thalamus

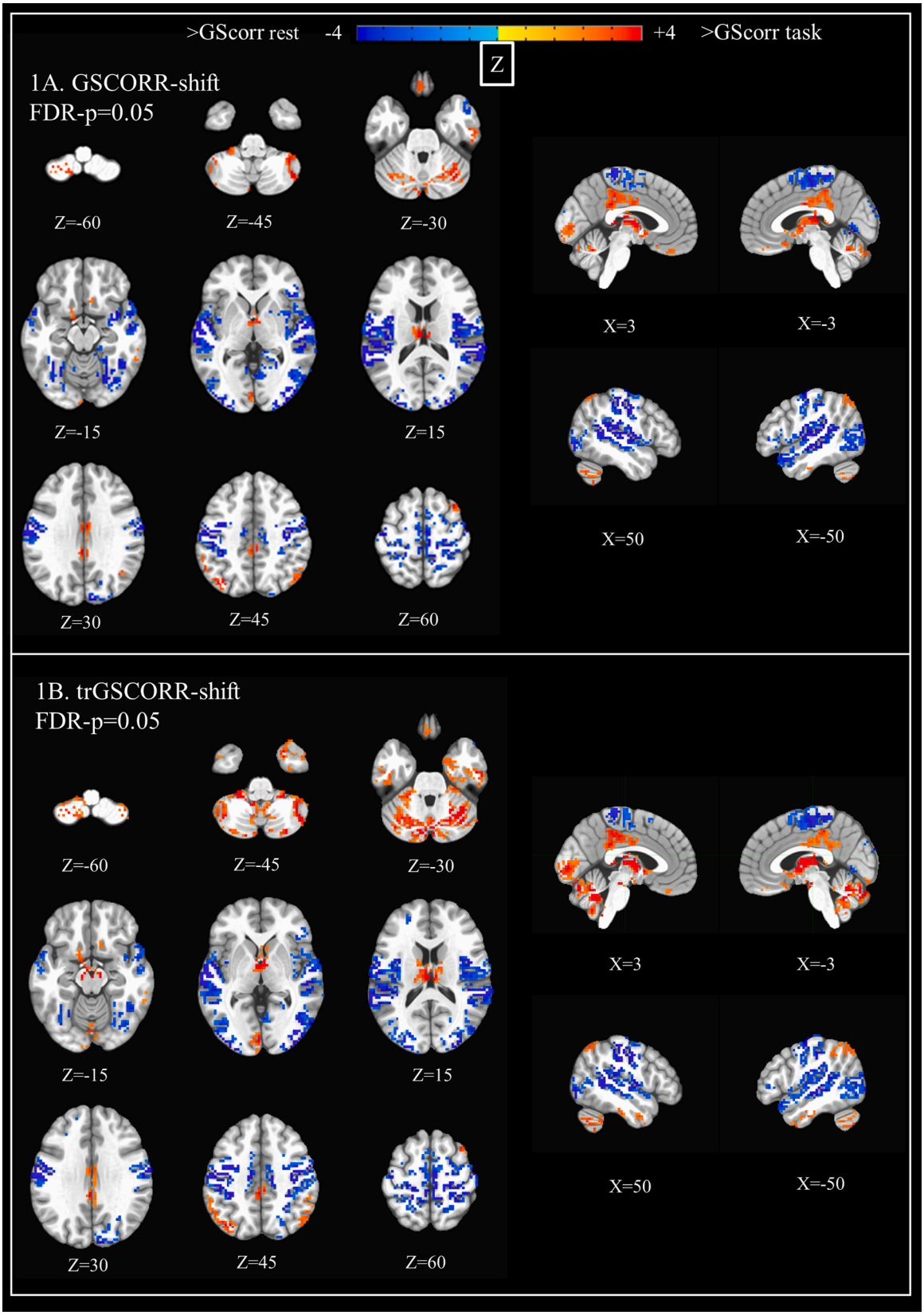

Fig. 1. GSCORR-shift and trGSCORR-shift maps. Whole brain, voxel-wise z maps displaying areas of significant differences at the paired *t*-test between: (A) GSCORR-task and GSCORR-rest (i.e. GSCORR-shift); (B) GSCORR-tr and GSCORR-rest (i.e. trGSCORR-shift).

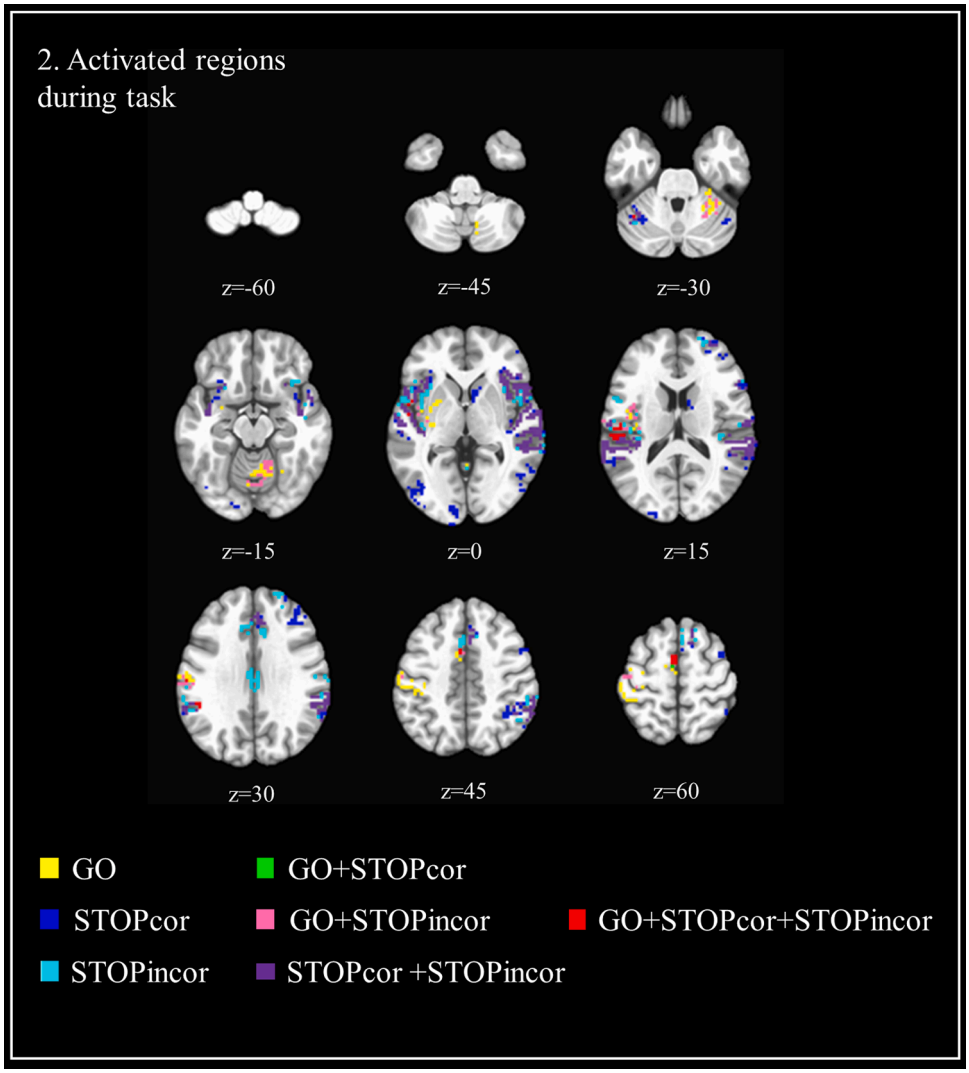

Fig. 2. BOLD activation map during stop-signal task. Whole brain, voxel-wise map showing areas activating during the stop-signal trials (GO, STOP correct and STOP incorrect, FDR-p = 0.05). Red regions are the ones exhibiting activation across all the three trias.

and cerebellum) and cortical regions (dPCC and PLPC) during the stop-signal task. The thalamus, as a gateway to the cortex, plays a crucial role in cognitive control, regulation of thoughts and actions, and goal-directed behaviors (Hwang and D'Esposito, 2022). The cerebellum, traditionally known for its role in motor coordination, has been increasingly recognized for its involvement in cognitive, behavioral processes and to play a role in cognition, emotion, and autonomic function (Rapoport et al., 2000; Schmahmann, 2019). PLPC is a higher-level association area, suggested to play a role in the executive control of attention, sensory integration and problem solving (Marek and Dosenbach, 2018; Middag-van Spanje et al., 2022; Thomson and Jaque, 2017). Finally, dPCC is one of the most important functional hubs belonging to the default mode network (Leech and Sharp, 2014), which was found to be associated with an increased metabolism during cognitive tasks (Rogan et al., 2022), rapid adjustments to visuospatial needs (Vogt and Palomero-Gallagher, 2012) and the modulation of attentional focus (Leech and Sharp, 2014). Considering these two opposite patterns, a reallocation of resources from sensory to associative regions during the execution of this attention-demanding task can be postulated. This hypothesis is further supported by previous evidence suggesting that at rest - when associative areas are less recruited than during tasks - GSCORR values are higher in sensory than associative regions (Liu et al., 2018; Yang et al., 2016; Zhang et al., 2020).

In the next chapter we will delve deeper into the relationship between GSCORR and brain activation by exploring the functional relationships between the regions with positive GSCORR-shift and those that were activated during the task.

4.2. *Task-related BOLD changes*

The current analysis revealed two well-distinguished clusters of BOLD task-related changes, one for the GO-baseline and one for the STOP(cor/incor)-baseline contrast, as previously observed (Zhang and Li, 2012a). These clusters are evident in both activation and deactivation maps and show opposite directions. Despite the many overlaps between STOPcor and STOPincor maps, very limited overlaps were found between GO and STOPcor maps, reflecting the presence of two separate systems operating for the response elicitation and inhibition. A few overlaps were found, however, between GO and STOPincor maps. This may reflect the fact that, during STOPincor trials, inhibition was not efficient and could not avoid the elicitation of the motor system.

Specifically, two regions (left-pre SMA and left IPL) were activated across the three task conditions. The novelty of the present findings resides in the observation of task>rest contrasts, while the majority of the literature reports comparisons between the trial conditions (e.g. STOPcor>STOPincor contrasts). However, we know from the available

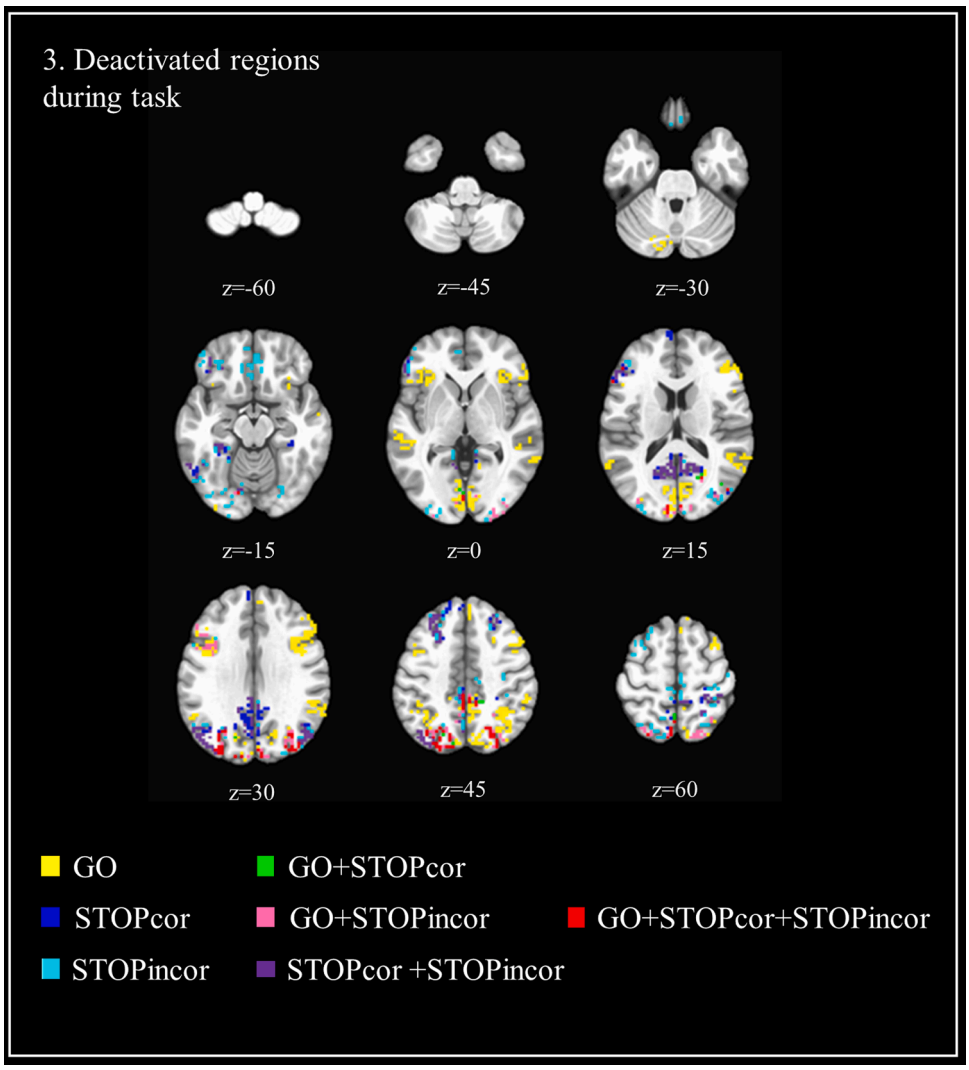

Fig. 3. BOLD deactivation map during stop-signal task. Whole brain, voxel-wise map showing areas exhibiting deactivation during the stop-signal trials (GO, STOP correct and STOP incorrect, FDR-p = 0.05). Red regions are the ones exhibiting deactivation across all the three trials.

Table 1A
Correlation maps between GSCORR and beta coefficients in the mask of regions showing *activation* across the three different trial conditions (n = 107).

Whole brain, voxel-wise significant regions		GSCORR-shift	GSCORR-rest	GSCORR-task
GO trials beta coefficients	r	0.095	−0.087	0.010
	p value	0.334	0.373	0.923
	p value corr	1.000	1.000	1.000
STOPcor trials beta coefficients	r	**0.245***	−0.128	0.125
	p value	0.011	0.192	0.201
	p value corr	1.000	1.000	1.000
STOPincor trials beta coefficients	r	0.109	−0.006	0.108
	p value	0.267	0.953	0.271
	p value corr	1.000	1.000	1.000

r = Pearson correlation coefficient; p value= uncorrected p value; p value corr= Bonferroni correction for multiple comparison; Shift=task-rest difference; STOPcor= Stop correct; STOPincor= STOP incorrect
* uncorrected p value<0.05.

Table 1B
Correlation maps between GSCORR and beta coefficients in the mask of regions showing *deactivation* across the three different trial conditions (n = 107).

Whole brain, voxel-wise significant regions		GSCORR-shift	GSCORR-rest	GSCORR-task
GO trials beta coefficients	r	−0.093	**−0.210***	**−0.299****
	p value	0.343	0.031	0.002
	p value corr	0.686	0.186	0.018
STOPcor trials beta coefficients	r	−0.121	−0.152	**−0.273****
	p value	0.215	0.119	0.005
	p value corr	0.645	0.476	0.040
STOPincor trials beta coefficients	r	0.035	**−0.241***	**−0.198***
	p value	0.725	0.013	0.042
	p value corr	0.725	0.091	0.210

r = Pearson correlation coefficient; p value= uncorrected p value; p value corr= Bonferroni correction for multiple comparison; Shift=task-rest difference; STOPcor= Stop correct; STOPincor= STOP incorrect
* uncorrected p value<0.05
** Bonferroni correction p value<0.05

evidence that SMA has been linked to performance-monitoring and the dynamic update of motor schemes (Cao and Cannon, 2021; Fauth-Bühler et al., 2012; Hughes et al., 2013), while IPL influences working memory and response inhibition (Chambers et al., 2009; Ray Li et al., 2006). Although some studies identified IPL and pre-SMA as part of the inhibition circuit activated during STOPcor trials, other studies observed that the involvement of this network goes beyond inhibition, as it is also recruited during positive behavioral responses (GO trials). The presence of BOLD-changes within the same regions (i.e. IPL and SMA) during both GO and STOP trials suggests that a common neural network may intervene in the phase immediately following the appearance of the first signal, when the subject is still uncertain about whether to press the button (GO trial) or inhibit the response (STOP trial) (Chikazoe et al., 2009).

4.2.1. Activation and GSCORR

Turning the attention to the GSCORR-activation relationship, the regions exhibiting a significant positive GSCORR-shift were not the same showing an activation throughout the task (eFig. 4). This is because GSCORR-shift and BOLD task-related changes provide information on different neurofunctional domains. A positive GSCORR-shift identifies regions whose activity becomes more prominent on the global signal during task execution, regardless of the specific type of trial. Thus, GSCORR-shift reflects a process that occurs across trial-types because this very process does not depend on the specific trial, but on the fact that the subject is in a *task-oriented* state. Activation, on the other hand, appears to be a trial-dependent measure, identifying regions that respond to specific stimuli such as GO or STOP prompts. Additionally, GSCORR-shift includes all the time points in the rest and task runs, while activation compares the stimulus-induced signal with the “rest” BOLD values of the intertrial interval. However, this rest period is different from the one observed during a resting-state run, as it could be considered a "task-oriented state" where the subject reflects on a recently completed trial and expects further prompts. Coherently with this hypothesis, no significant correlation between GSCORR (rest/task/shift) and activation (GO/STOPcor/STOPincor) was observed.

The presence of a task-oriented state is further confirmed by the fact that the GSCORR-shift findings are topographically similar, although further enhanced, when using task residuals. In trGSCORR-shift, the activity related to single trials is indeed regressed out. In fact, task residual activity can be considered as the spontaneous signals during a task state. In light of these results, GSCORR mirrors the task-engagement, that is, the predisposition of the individual to react to task-related stimuli (Zhang and Li, 2010, 2012b). The behavioral relevance of such attentional shift from rest to task is supported by the fact that correlation analyses with performance indices (i.e., SSRT and RT) identified behavioral correlates of GSCORR (eFigs. 2 and 3).

4.2.2. Deactivation and GSCORR

Although the information from previous literature is too scarce to allow direct comparisons, it is noteworthy that deactivation displays stronger correlations with GSCORR compared to activation. Specifically, during the task, areas showing deactivation are more functionally correlated with the global signal. There are at least two possible explanations for this association. Firstly, one of the most important theories about negative beta-coefficients describes them as the result of local neural inhibition (Sten et al., 2017). Therefore, specific areas may require local inhibition in order to increase their global connectivity. Secondly, the increased global connectivity of a region implies that this region is more influenced by distant areas that, in our specific case, may be inhibitory. Future studies on the interplay between local and global connectivity are required to shed further light on these intriguing possibilities.

A last but fundamental observation can be derived from our sensitivity analyses. In fact, GSCORR-shift pattern after GSR was not only reduced, but also complementary to the map observed without GSR (eFig. 1). These findings are consistent with the hypothesis advocating for the informative nature of the global signal (Scalabrini et al., 2020b; Zhang et al., 2020). Besides, they confirm that inclusion and exclusion of GSR are two potentially complementary preprocessing methods whose use depends on the specific research questions (Murphy and Fox, 2017).

4.3. Future directions

GSCORR assesses the strength of association between regional brain activity and the global signal. However, recent studies focused instead on characterizing the temporal dynamics underlying the association between local and global connectivity in fMRI analyses (Amemiya et al., 2014; Kavroulakis et al., 2021; Lv et al., 2013; Mitra et al., 2014). This approach is defined as time-shift analysis or lag-structure analysis (Mitra et al., 2014) and explores how local-to-global correlations change when shifting the lag between the local and the global timeseries. As GSCORR can be defined as a zero-lag time-shift analysis, the present study lays the groundwork to better interpret task-related activation/deactivation when taking into account the temporal structure of brain dynamics.

In light of the magnitude of the GSCORR findings for the stop-signal task, we also expect this brain dynamic to be characteristic of all the conditions requiring a continuous engagement. Future studies may try to replicate the present findings in other tasks that are more intermittent or less attentionally demanding in order to test whether GSCORR-shift is subject to similar changes or not. These observations would further help to differentiate trial-independent modulations from trial-dependent ones.

4.4. Limitations

Although the main dataset on which analyses were performed was of high quality, no other sample available online included both rest and stop-signal task runs. Therefore, the replicability of the present findings could not be tested. The replication crisis is well documented in psychology and psychiatry and requires collaborative efforts to ensure data sharing and harmonized infrastructures (Salazar de Pablo et al., 2021).

This study primarily provides correlational data, thereby restricting our capacity to infer causality between GSCORR and changes in task-related activation/deactivation. Future studies could delve into the contribution of connectivity measures to task-related BOLD changes, for example, by employing linear regression models (Yuan et al., 2013). In particular, we found a significant correlation between GSCORR and deactivation, whose causal relationship could yield interesting results.

Of note, these results are not generalizable to the task condition in general, as our analyses exclusively focused on a specific type of task (i.e., the stop-signal). Predicting the outcomes of analyses applied to tasks beyond the stop-signal task presents a challenge, compounded by the scant literature on the GSCORR-task (and GSCORR-shift) measures. Zhang et al. identified a consistent pattern of GSCORR-shift across seven diverse tasks (emotional, reward-learning, language, motor, relational reasoning, social cognition, visual N-back), calling for the involvement of GSCORR-shift not only across trials within the same task, but also across tasks (Zhang et al., 2020).

As discussed in Section 2.7, the interpretation of our results must acknowledge the limitations associated with the use of "global signal" approaches. For this reason, we have presented the results both with and without GSR (Murphy and Fox, 2017; Shirer et al., 2015).

5. Conclusions

The state-dependent reconfiguration of GSCORR suggests a reallocation of functional resources to associative areas during a stop-signal task. Findings showed that GSCORR and task-related BOLD changes (i.e. activation and deactivation) represent distinct neurofunctional proxies of brain activity, shedding new light about the functional meaning of deactivation.

6. Disclosure statement

6.1. Funding sources

This research received no specific grant from any funding agency in the public, commercial, or not-for-profit sectors.

7. Compliance with ethical standards

This study used a shared neuroimaging dataset from the UCLA Consortium for Neuropsychiatric Phenomics, all analyses conformed with the ethical standards as laid down in the 1964 Declaration of Helsinki and its later amendments.

Data and code availability statement

Original fMRI data was obtained from the OpenfMRI database (https://openfmri.org/dataset/ds000030/); its accession number is ds000030. AFNI scripts used to analyze fMRI data and the data that support the findings of this study are available from the corresponding author, PLTV, upon reasonable request and can be used for other works by including the first authors of this article as co-authors of the work. Activation/deactivation maps for all task conditions have been provided as NIFTI files in the supplementary materials and can be used for other works by including the first authors of this article as co-authors of the work.

CRediT authorship contribution statement

Stefano Damiani: Writing – original draft, Visualization, Validation, Methodology, Formal analysis, Data curation, Conceptualization. **Paolo La-Torraca-Vittori:** Writing – original draft, Visualization, Validation, Methodology, Formal analysis, Data curation, Conceptualization. **Livio Tarchi:** Writing – original draft, Methodology, Formal analysis. **Eleonora Tosi:** Formal analysis. **Valdo Ricca:** Writing – review & editing, Supervision. **Andrea Scalabrini:** Writing – review & editing, Methodology. **Pierluigi Politi:** Writing – review & editing, Supervision. **Paolo Fusar-Poli:** Writing – review & editing, Supervision.

Declaration of competing interest

The authors declare no conflict of interest.

Data availability

Data will be made available on request.

Acknowledgments

This data was obtained from the OpenfMRI database (https://openfmri.org/dataset/ds000030/). Its accession number is ds000030. The Authors would like to thank the investigators who shared the UCLA dataset: Bilder, R, Poldrack, R, Cannon, T, London, E, Freimer, N, Congdon, E, Karlsgodt, K, Sabb, F.

Paolo Fusar-Poli was supported by #NEXTGENERATIONEU (NGEU) from the Ministry of University and Research (MUR), National Recovery and Resilience Plan (NRRP), project MNESYS (PE0000006) – A Multiscale integrated approach to the study of the nervous system in health and disease (DN. 1553 11.10.2022).

Supplementary materials

Supplementary material associated with this article can be found, in the online version, at doi:10.1016/j.neuroimage.2024.120585.

References

Allison, J.D., Meador, K.J., Loring, D.W., Figueroa, R.E., Wright, J.C., 2000. Functional MRI cerebral activation and deactivation during finger movement. Neurology 54, 135–142. https://doi.org/10.1212/wnl.54.1.135.

Amemiya, S., Kunimatsu, A., Saito, N., Ohtomo, K., 2014. Cerebral hemodynamic impairment: assessment with resting-state functional MR imaging. Radiology 270, 548–555. https://doi.org/10.1148/radiol.13130982.

Ao, Y., Ouyang, Y., Yang, C., Wang, Y., 2021. Global signal topography of the human brain: a novel framework of functional connectivity for psychological and pathological investigations. Front. Hum. Neurosci. 15, 644892 https://doi.org/10.3389/fnhum.2021.644892.

Band, G.P.H., van der Molen, M.W., Logan, G.D., 2003. Horse-race model simulations of the stop-signal procedure. Acta Psychol. 112, 105–142. https://doi.org/10.1016/S0001-6918(02)00079-3 (Amst.).

Bowring, A., Maumet, C., Nichols, T.E., 2021. Erratum: exploring the impact of analysis software on task fMRI results. Hum. Brain Mapp. 42, 1564–1578. https://doi.org/10.1002/hbm.25302.

Buzsáki, G., Kaila, K., Raichle, M., 2007. Inhibition and brain work. Neuron 56, 771–783. https://doi.org/10.1016/j.neuron.2007.11.008.

Caballero-Gaudes C., Reynolds R.C., 2017. Methods for cleaning the BOLD fMRI signal. NeuroImage, Cleaning up the fMRI time series: mitigating noise with advanced acquisition and correction strategies 154, 128–149. 10.1016/j.neuroimage.2016.12.018.

Cao, H., Cannon, T.D., 2021. Distinct and temporally associated neural mechanisms underlying concurrent, postsuccess, and posterror cognitive controls: evidence from a stop-signal task. Hum. Brain Mapp. 42, 2677–2690. https://doi.org/10.1002/hbm.25347.

Chai, X.J., Castañón, A.N., Ongür, D., Whitfield-Gabrieli, S., 2012. Anticorrelations in resting state networks without global signal regression. Neuroimage 59, 1420–1428. https://doi.org/10.1016/j.neuroimage.2011.08.048.

Chambers, C.D., Garavan, H., Bellgrove, M.A., 2009. Insights into the neural basis of response inhibition from cognitive and clinical neuroscience. Neurosci. Biobehav. Rev. 33, 631–646. https://doi.org/10.1016/j.neubiorev.2008.08.016.

Chikazoe, J., Jimura, K., Hirose, S., Yamashita, K., Miyashita, Y., Konishi, S., 2009. Preparation to inhibit a response complements response inhibition during performance of a stop-signal task. J. Neurosci. 29, 15870–15877. https://doi.org/10.1523/JNEUROSCI.3645-09.2009.

Choe, A.S., Jones, C.K., Joel, S.E., Muschelli, J., Belegu, V., Caffo, B.S., Lindquist, M.A., Van Zijl, P.C.M., Pekar, J.J., 2015. Reproducibility and temporal structure in weekly resting-state fMRI over a period of 3.5 years. PLoS One 10, e0140134. https://doi.org/10.1371/journal.pone.0140134.

Cole, M.W., Bassett, D.S., Power, J.D., Braver, T.S., Petersen, S.E., 2014. Intrinsic and task-evoked network architectures of the human brain. Neuron 83, 238–251. https://doi.org/10.1016/j.neuron.2014.05.014.

Cole, M.W., Ito, T., Bassett, D.S., Schultz, D.H., 2016. Activity flow over resting-state networks shapes cognitive task activations. Nat. Neurosci. 19, 1718–1726. https://doi.org/10.1038/nn.4406.

Cole, M.W., Ito, T., Schultz, D., Mill, R., Chen, R., Cocuzza, C., 2019. Task activations produce spurious but systematic inflation of task functional connectivity estimates. Neuroimage 189, 1–18. https://doi.org/10.1016/j.neuroimage.2018.12.054.

Cox, R.W., 1996. AFNI: software for analysis and visualization of functional magnetic resonance neuroimages. Comput. Biomed. Res. Int. J. 29, 162–173. https://doi.org/10.1006/cbmr.1996.0014.

Cox, R.W., Hyde, J.S., 1997. Software tools for analysis and visualization of fMRI data. NMR Biomed. 10, 171–178. https://doi.org/10.1002/(sici)1099-1492(199706/08)10:4/5<171::aid-nbm453>3.0.co;2-l.

Damiani, S., Tarchi, L., La-Torraca-Vittori, P., Scalabrini, A., Castellini, G., Ricca, V., Fusar-Poli, P., Politi, P., 2022. State-dependent reductions of local brain connectivity in schizophrenia and their relation to performance and symptoms: a functional magnetic resonance imaging study. Psychiatry Res. Neuroimaging 326, 111541. https://doi.org/10.1016/j.pscychresns.2022.111541.

Devor, A., Hillman, E.M.C., Tian, P., Waeber, C., Teng, I.C., Ruvinskaya, L., Shalinsky, M. H., Zhu, H., Haslinger, R.H., Narayanan, S.N., Ulbert, I., Dunn, A.K., Lo, E.H., Rosen, B.R., Dale, A.M., Kleinfeld, D., Boas, D.A., 2008. Stimulus-induced changes in blood flow and 2-deoxyglucose uptake dissociate in ipsilateral somatosensory cortex. J. Neurosci. 28, 14347–14357. https://doi.org/10.1523/JNEUROSCI.4307-08.2008.

Fair, D.A., Schlaggar, B.L., Cohen, A.L., Miezin, F.M., Dosenbach, N.U.F., Wenger, K.K., Fox, M.D., Snyder, A.Z., Raichle, M.E., Petersen, S.E., 2007. A method for using blocked and event-related fMRI data to study "resting state" functional connectivity. Neuroimage 35, 396–405. https://doi.org/10.1016/j.neuroimage.2006.11.051.

Fauth-Bühler, M., de Rover, M., Rubia, K., Garavan, H., Abbott, S., Clark, L., Vollstädt-Klein, S., Mann, K., Schumann, G., Robbins, T.W., 2012. Brain networks subserving fixed versus performance-adjusted delay stop trials in a stop signal task. Behav. Brain Res. 235, 89–97. https://doi.org/10.1016/j.bbr.2012.07.023.

Fox, M.D., Snyder, A.Z., Vincent, J.L., Corbetta, M., Essen, D.C.V., Raichle, M.E., 2005. The human brain is intrinsically organized into dynamic, anticorrelated functional networks. Proc. Natl. Acad. Sci. 102, 9673–9678. https://doi.org/10.1073/pnas.0504136102.

Fox, M.D., Zhang, D., Snyder, A.Z., Raichle, M.E., 2009. The global signal and observed anticorrelated resting state brain networks. J. Neurophysiol. 101, 3270–3283. https://doi.org/10.1152/jn.90777.2008.

Gorgolewski, K.J., Durnez, J., Poldrack, R.A., 2017. Preprocessed consortium for neuropsychiatric phenomics dataset. F1000Res. 6, 1262. https://doi.org/10.12688/f1000research.11964.2.

Hamzei, F., Dettmers, C., Rzanny, R., Liepert, J., Büchel, C., Weiller, C., 2002. Reduction of excitability ("inhibition") in the ipsilateral primary motor cortex is mirrored by fMRI signal decreases. Neuroimage 17, 490–496. https://doi.org/10.1006/nimg.2002.1077.

Harel, N., Lee, S.P., Nagaoka, T., Kim, D.S., Kim, S.G., 2002. Origin of negative blood oxygenation level-dependent fMRI signals. J. Cereb. Blood Flow Metab. Off. J. Int. Soc. Cereb. Blood Flow Metab. 22, 908–917. https://doi.org/10.1097/00004647-200208000-00002.

Hughes, M.E., Johnston, P.J., Fulham, W.R., Budd, T.W., Michie, P.T., 2013. Stop-signal task difficulty and the right inferior frontal gyrus. Behav. Brain Res. 256, 205–213. https://doi.org/10.1016/j.bbr.2013.08.026.

Hwang, K., D'Esposito, M., Halassa, M.M., 2022. The thalamus in cognitive control. The Thalamus. Cambridge University Press, pp. 307–323. https://doi.org/10.1017/9781108674287.017.

Jo, H.J., Saad, Z.S., Simmons, W.K., Milbury, L.A., Cox, R.W., 2010. Mapping sources of correlation in resting state FMRI, with artifact detection and removal. Neuroimage 52, 571–582. https://doi.org/10.1016/j.neuroimage.2010.04.246.

Kannurpatti, S.S., Biswal, B.B., 2004. Negative functional response to sensory stimulation and its origins. J. Cereb. Blood Flow Metab. 24, 703–712. https://doi.org/10.1097/01.WCB.0000121232.04853.46.

Kavroulakis, E., Simos, N.J., Maris, T.G., Zaganas, I., Panagiotakis, S., Papadaki, E., 2021. Evidence of age-related hemodynamic and functional connectivity impairment: a resting state fMRI study. Front. Neurol. 12, 633500 https://doi.org/10.3389/fneur.2021.633500.

Konstantareas, M.M., Hewitt, T., 2001. Autistic disorder and schizophrenia: diagnostic overlaps. J. Autism Dev. Disord. 31, 19–28. https://doi.org/10.1023/A:1005605528309.

Leech, R., Sharp, D.J., 2014. The role of the posterior cingulate cortex in cognition and disease. Brain 137, 12–32. https://doi.org/10.1093/brain/awt162.

Li, W., Zhou, F.C., Zhang, L., Ng, C.H., Ungvari, G.S., Li, J., Xiang, Y.T., 2020. Comparison of cognitive dysfunction between schizophrenia and bipolar disorder patients: a meta-analysis of comparative studies. J. Affect. Disord. 274, 652–661. https://doi.org/10.1016/j.jad.2020.04.051.

Liu, X., De Zwart, J.A., Schölvinck, M.L., Chang, C., Ye, F.Q., Leopold, D.A., Duyn, J.H., 2018. Subcortical evidence for a contribution of arousal to fMRI studies of brain activity. Nat. Commun. 9, 395. https://doi.org/10.1038/s41467-017-02815-3.

Logan, G.D., Cowan, W.B., 1984. On the ability to inhibit thought and action: a theory of an act of control. Psychol. Rev. 91, 295–327. https://doi.org/10.1037/0033-295X.91.3.295.

Lv, Y., Margulies, D.S., Cameron Craddock, R., Long, X., Winter, B., Gierhake, D., Endres, M., Villringer, K., Fiebach, J., Villringer, A., 2013. Identifying the perfusion deficit in acute stroke with resting-state functional magnetic resonance imaging. Ann. Neurol. 73, 136–140. https://doi.org/10.1002/ana.23763.

Ma, S., Calhoun, V.D., Eichele, T., Du, W., Adalı, T., 2012. Modulations of functional connectivity in the healthy and schizophrenia groups during task and rest. Neuroimage 62, 1694–1704. https://doi.org/10.1016/j.neuroimage.2012.05.048.

Marek, S., Dosenbach, N.U.F., 2018. The frontoparietal network: function, electrophysiology, and importance of individual precision mapping. Dialogues Clin. Neurosci. 20, 133–140. https://doi.org/10.31887/DCNS.2018.20.2/smarek.

Middag-van Spanje, M., Duecker, F., Gallotto, S., de Graaf, T.A., van Heugten, C., Sack, A. T., Schuhmann, T., 2022. Transcranial magnetic stimulation over posterior parietal cortex modulates alerting and executive control processes in attention. Eur. J. Neurosci. 56, 5853–5868. https://doi.org/10.1111/ejn.15830.

Mitra, A., Snyder, A.Z., Hacker, C.D., Raichle, M.E., 2014. Lag structure in resting-state fMRI. J. Neurophysiol. 111, 2374–2391. https://doi.org/10.1152/jn.00804.2013.

Murphy, K., Fox, M.D., 2017. Towards a consensus regarding global signal regression for resting state functional connectivity MRI. Neuroimage 154, 169–173. https://doi.org/10.1016/j.neuroimage.2016.11.052.

Nakata, H., Domoto, R., Mizuguchi, N., Sakamoto, K., Kanosue, K., 2019. Negative BOLD responses during hand and foot movements: an fMRI study. PLoS One 14, e0215736. https://doi.org/10.1371/journal.pone.0215736.

Poldrack, R.A., Congdon, E., Triplett, W., Gorgolewski, K.J., Karlsgodt, K.H., Mumford, J. A., Sabb, F.W., Freimer, N.B., London, E.D., Cannon, T.D., Bilder, R.M., 2016. A phenome-wide examination of neural and cognitive function. Sci. Data 3, 160110. https://doi.org/10.1038/sdata.2016.110.

Power, J.D., Mitra, A., Laumann, T.O., Snyder, A.Z., Schlaggar, B.L., Petersen, S.E., 2014. Methods to detect, characterize, and remove motion artifact in resting state fMRI. Neuroimage 84, 320–341. https://doi.org/10.1016/j.neuroimage.2013.08.048.

Power, J.D., Plitt, M., Laumann, T.O., Martin, A., 2017. Sources and implications of whole-brain fMRI signals in humans. Neuroimage 146, 609–625. https://doi.org/10.1016/j.neuroimage.2016.09.038.

Qin, P., Wang, M., Northoff, G., 2020. Linking bodily, environmental and mental states in the self-A three-level model based on a meta-analysis. Neurosci. Biobehav. Rev. 115, 77–95. https://doi.org/10.1016/j.neubiorev.2020.05.004.

Rapoport, M., van Reekum, R., Mayberg, H., 2000. The role of the cerebellum in cognition and behavior: a selective review. J. Neuropsychiatry Clin. Neurosci. 12, 193–198. https://doi.org/10.1176/jnp.12.2.193.

Ray Li, C., Huang, C., Constable, R.T., Sinha, R., 2006. Imaging response inhibition in a stop-signal task: neural correlates independent of signal monitoring and post-response processing. J. Neurosci. 26, 186–192. https://doi.org/10.1523/JNEUROSCI.3741-05.2006.

Rogan, M., Friend, A.T., Rossetti, G.M., Edden, R., Mikkelsen, M., Oliver, S.J., Macdonald, J.H., Mullins, P.G., 2022. Hypoxia alters posterior cingulate cortex metabolism during a memory task: a 1H fMRS study. Neuroimage 260, 119397. https://doi.org/10.1016/j.neuroimage.2022.119397.

Rogers, B.P., Morgan, V.L., Newton, A.T., Gore, J.C., 2007. Assessing functional connectivity in the human brain by fMRI. Magn. Reson. Imaging 25, 1347–1357. https://doi.org/10.1016/j.mri.2007.03.007.

Saad, Z.S., Glen, D.R., Chen, G., Beauchamp, M.S., Desai, R., Cox, R.W., 2009. A new method for improving functional-to-structural MRI alignment using local pearson correlation. Neuroimage 44, 839–848. https://doi.org/10.1016/j.neuroimage.2008.09.037.

Sadato, N., Pascual-Leone, A., Grafman, J., Deiber, M.P., Ibañez, V., Hallett, M., 1998. Neural networks for Braille reading by the blind. Brain J. Neurol. 121 (Pt 7), 1213–1229. https://doi.org/10.1093/brain/121.7.1213.

Sadato, N., Pascual-Leone, A., Grafman, J., Ibañez, V., Deiber, M.P., Dold, G., Hallett, M., 1996. Activation of the primary visual cortex by Braille reading in blind subjects. Nature 380, 526–528. https://doi.org/10.1038/380526a0.

Salazar de Pablo, G., Studerus, E., Vaquerizo-Serrano, J., Irving, J., Catalan, A., Oliver, D., Baldwin, H., Danese, A., Fazel, S., Steyerberg, E.W., Stahl, D., Fusar-Poli, P., 2021. Implementing precision psychiatry: a systematic review of individualized prediction models for clinical practice. Schizophr. Bull. 47, 284–297. https://doi.org/10.1093/schbul/sbaa120.

Satterthwaite, T.D., Elliott, M.A., Gerraty, R.T., Ruparel, K., Loughead, J., Calkins, M.E., Eickhoff, S.B., Hakonarson, H., Gur, R.C., Gur, R.E., Wolf, D.H., 2013. An improved framework for confound regression and filtering for control of motion artifact in the preprocessing of resting-state functional connectivity data. Neuroimage 64, 240–256. https://doi.org/10.1016/j.neuroimage.2012.08.052.

Scalabrini, A., Mucci, C., Esposito, R., Damiani, S., Northoff, G., 2020a. Dissociation as a disorder of integration – On the footsteps of Pierre Janet. Prog. Neuropsychopharmacol. Biol. Psychiatry 101, 109928. https://doi.org/10.1016/j.pnpbp.2020.109928.

Scalabrini, A., Vai, B., Poletti, S., Damiani, S., Mucci, C., Colombo, C., Zanardi, R., Benedetti, F., Northoff, G., 2020b. All roads lead to the default-mode network—Global source of DMN abnormalities in major depressive disorder. Neuropsychopharmacology 45, 2058–2069. https://doi.org/10.1038/s41386-020-0785-x.

Schmahmann, J.D., 2019. The cerebellum and cognition. Neurosci. Lett. 688, 62–75. https://doi.org/10.1016/j.neulet.2018.07.005.

Shirer, W.R., Jiang, H., Price, C.M., Ng, B., Greicius, M.D., 2015. Optimization of rs-fMRI pre-processing for enhanced signal-noise separation, test-retest reliability, and group discrimination. Neuroimage 117, 67–79. https://doi.org/10.1016/j.neuroimage.2015.05.015.

Shmuel, A., Yacoub, E., Pfeuffer, J., Van de Moortele, P.F., Adriany, G., Hu, X., Ugurbil, K., 2002. Sustained negative BOLD, blood flow and oxygen consumption response and its coupling to the positive response in the human brain. Neuron 36, 1195–1210. https://doi.org/10.1016/s0896-6273(02)01061-9.

Stefanovic, B., Warnking, J.M., Pike, G.B., 2004. Hemodynamic and metabolic responses to neuronal inhibition. Neuroimage 22, 771–778. https://doi.org/10.1016/j.neuroimage.2004.01.036.

Sten, S., Lundengård, K., Witt, S.T., Cedersund, G., Elinder, F., Engström, M., 2017. Neural inhibition can explain negative BOLD responses: a mechanistic modelling and fMRI study. Neuroimage 158, 219–231. https://doi.org/10.1016/j.neuroimage.2017.07.002.

Tanabe, S., Huang, Z., Zhang, Jun, Chen, Y., Fogel, S., Doyon, J., Wu, J., Xu, J., Zhang, Jianfeng, Qin, P., Wu, X., Mao, Y., Mashour, G.A., Hudetz, A.G., Northoff, G., 2020. Altered global brain signal during physiologic, pharmacologic, and pathologic states of unconsciousness in humans and rats. Anesthesiology 132, 1392–1406. https://doi.org/10.1097/ALN.0000000000003197.

Thomson, P., Jaque, S.V., 2017. Neurobiology, creativity, and Performing artists, in: Creativity and the Performing Artist. Elsevier, pp. 79–102. https://doi.org/10.1016/B978-0-12-804051-5.00006-8.

Tommasin, S., Mascali, D., Moraschi, M., Gili, T., Hassan, I.E., Fratini, M., DiNuzzo, M., Wise, R.G., Mangia, S., Macaluso, E., Giove, F., 2018. Scale-invariant rearrangement of resting state networks in the human brain under sustained stimulation. Neuroimage 179, 570–581. https://doi.org/10.1016/j.neuroimage.2018.06.006.

Tzourio-Mazoyer, N., Petit, L., Zago, L., Crivello, F., Vinuesa, N., Joliot, M., Jobard, G., Mellet, E., Mazoyer, B., 2015. Between-hand difference in ipsilateral deactivation is associated with hand lateralization: fMRI mapping of 284 volunteers balanced for handedness. Front. Hum. Neurosci. 9, 5. https://doi.org/10.3389/fnhum.2015.00005.

Verbruggen, F., Logan, G.D., 2009. Models of response inhibition in the stop-signal and stop-change paradigms. Neurosci. Biobehav. Rev. 33, 647–661. https://doi.org/10.1016/j.neubiorev.2008.08.014.

Verbruggen, F., Logan, G.D., 2008. Response inhibition in the stop-signal paradigm. Trends Cogn. Sci. 12, 418–424. https://doi.org/10.1016/j.tics.2008.07.005.

Vogt, B.A., Palomero-Gallagher, N., 2012. Cingulate cortex. The Human Nervous System. Elsevier, pp. 943–987. https://doi.org/10.1016/B978-0-12-374236-0.10025-2.

Vovk, A., Cox, R.W., Stare, J., Suput, D., Saad, Z.S., 2011. Segmentation priors from local image properties: without using bias field correction, location-based templates, or registration. Neuroimage 55, 142–152. https://doi.org/10.1016/j.neuroimage.2010.11.082.

Yang, G.J., Murray, J.D., Glasser, M., Pearlson, G.D., Krystal, J.H., Schleifer, C., Repovs, G., Anticevic, A., 2016. Altered global signal topography in schizophrenia. Cereb. Cortex Cercor bhw297v1. https://doi.org/10.1093/cercor/bhw297.

Yuan, R., Di, X., Kim, E.H., Barik, S., Rypma, B., Biswal, B.B., 2013. Regional homogeneity of resting-state fMRI contributes to both neurovascular and task activation variations. Magn. Reson. Imaging 31, 1492–1500. https://doi.org/10.1016/j.mri.2013.07.005.

Zeharia, N., Hertz, U., Flash, T., Amedi, A., 2012. Negative blood oxygenation level dependent homunculus and somatotopic information in primary motor cortex and

supplementary motor area. Proc. Natl. Acad. Sci. U. S. A. 109, 18565–18570. https://doi.org/10.1073/pnas.1119125109.

Zhang, J., Huang, Z., Tumati, S., Northoff, G., 2020. Rest-task modulation of fMRI-derived global signal topography is mediated by transient coactivation patterns. PLOS Biol. 18, e3000733 https://doi.org/10.1371/journal.pbio.3000733.

Zhang, S., Li, C.R., 2012a. Functional networks for cognitive control in a stop signal task: independent component analysis. Hum. Brain Mapp. 33, 89–104. https://doi.org/10.1002/hbm.21197.

Zhang, S., Li, C.R., 2010. A neural measure of behavioral engagement: task-residual low-frequency blood oxygenation level-dependent activity in the precuneus. Neuroimage 49, 1911–1918. https://doi.org/10.1016/j.neuroimage.2009.09.004.

Zhang, S., Li, C.S.R., 2012b. Task-related, low-frequency task-residual, and resting state activity in the default mode network brain regions. Front. Psychol. 3 https://doi.org/10.3389/fpsyg.2012.00172.

Zhu, W., Che, Y., Wang, Y., Jia, Z., Wan, T., Wen, J., Cheng, J., Ren, C., Wu, J., Li, Y., Wang, Q., 2019. Study on neuropathological mechanisms of primary monosymptomatic nocturnal enuresis in children using cerebral resting-state functional magnetic resonance imaging. Sci. Rep. 9, 19141. https://doi.org/10.1038/s41598-019-55541-9.